

Development of Polar Geomagnetic Disturbance and PCA Event on February 11, 1958

By

M. NAGAI

Magnetic Observatory, Kakioka, Ibaraki, Japan

and

Y. HAKURA

The Radio Research Laboratories, Tokyo, Japan

Abstract

An investigation was made on the development of ionospheric and geomagnetic storms caused by solar corpuscular clouds emitted from a major flare that appeared at 21 : 08 UT on February 9, 1958.

Several interesting characteristics are discussed in the present analysis on the relation between the world-wide patterns of ionospheric disturbances and the corresponding current systems of geomagnetic storms, such as simultaneous occurrence of a peculiar polar disturbance with sudden development of PCA in the auroral zone far preceding the sudden commencement and appearance of the transient stage removed from S_p^+ -field to DP(Pre SC)-field, unusual increase of ionization right before the onset of the sudden commencement over the whole polar cap, outstanding two-stepped expansions of the region of polar cap blackouts and equivalent current systems of two successive sudden commencements, and variations of directions of the straight currents flowing in the central part of the polar cap.

§ 1. Introduction

A great magnetic storm occurred on February 11, 1958 with its sudden commencement at 01 : 26 UT. The magnetic storm was unusually on a large scale and accompanied with a cosmic ray storm, intense aurora, polar blackouts, storm Es, and F_2 layer disturbances of peculiar feature. Thus, in various fields deep interest has been concentrated on this event, and until now a number of research papers have been published in discussion about many interesting aspects of the disturbance.

In the earlier paper, we already clarified several important characteristics of the event, especially in the field of solar cosmic ray effect on the earth's polar

ionosphere. The existence of PCA (Polar Cap Absorption) was first detected on the world-wide analysis of ionospheric sounding data (Hakura, et al., 1958). The importance of solar radio outbursts of type IV for occurrence of PCA was recognized through a statistical examination of solar-geophysical data (Hakura and Goh, 1959). On the general theory of the earth storm, the progressive patterns of PCA event were explained from somewhat wider view of the solar-terrestrial relationship (Obayashi and Hakura, 1960-a and -b). Another important characteristic of PCA is its simultaneous occurrence with a polar geomagnetic disturbance which preceded the onset of sudden commencement on Feb. 11, 1958 (Nagai, 1964).

However, the research papers in other fields have revealed more and more complicated features of the events. New facts thus clarified urge us to do further research in the detailed structure of the disturbance. In the present paper, an attempt is made to reexamine several interesting aspects on the development of ionospheric and geomagnetic storms caused by solar corpuscular clouds emitted from a flare of importance 2+ followed by the type IV outburst that appeared at the center of the solar disk at 21 : 08 UT on Feb. 9, 1958.

In the second section, the development of impact zone of solar cosmic rays is discussed on the examination of progressive pattern of the PCA region. At this stage, a sudden development of PCA occurred in the auroral zone, in association with a peculiar type of polar magnetic disturbance. The third section deals with an unusual increase of PCA right before the sudden commencement which was originally discussed by Axford and Reid (1962). Immediately after two successive sudden commencements of the geomagnetic storm, the entire world was covered by severe disturbances of the polar origin. The fourth section treats the problem in view of the simultaneous boundary changes of the events, concerned with the distortion of the earth's magnetosphere at the attainment of shock waves responsible for the SC's. And in the fifth section, the directions of the straight currents in the central part of the polar cap in whole stages of the magnetic storm are analysed, as our final topic.

§ 2. Sudden development of PCA in the auroral zone and associated polar magnetic disturbance far before the sudden commencement.....(PCA)_A and DP (pre SC)

In order to observe the development patterns of PCA, Fig. 1 gives the storm-time change of Δf min in the polar region (a) and in the auroral zone (b). Here, Δf min means an average value of Δf min's at several selected stations, so that it

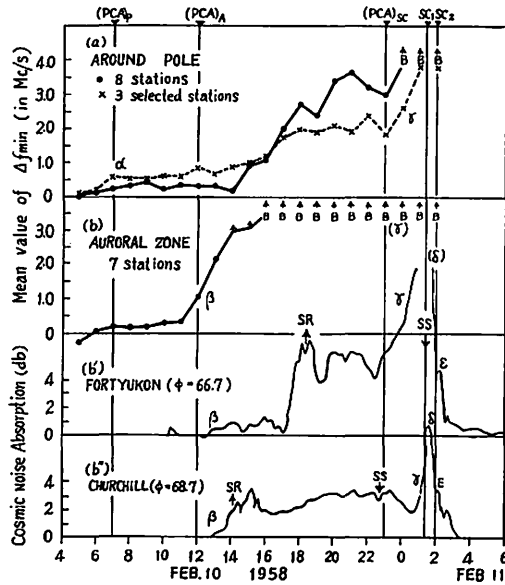


Fig. 1 Development of PCA around the pole (a) and in the auroral zone (b,b',b'')

- (a) Mean value of Δf min at 8 polar stations : Thule, Eureka, Alert, Fletchers. Ice, Resolute Bay, Clyde River, Godhavn, and Arctic II (thick line).
 × : Mean value of Δf min at 3 stations of solar side : Alert, Godhavn and Arctic II (thin line)
- (b) Mean value of Δf min at 7 stations : Tromsø, Dixon Is., Arctic 1, Point Barrow, Churchill, Narsarsuaq, and Reykjavik.
- (b'), (b'') Cosmic noise absorption at Fort Yukon (27.6 MC/s) and Churchill (30.0 MC/s). (after Axford and Reid, 1962).
 SR : Sunrise, SS : Sunset.

gives a kind of Dst-variation of polar cap absorption. For comparison, it also gives the time change of cosmic noise absorptions observed by riometers at two auroral zone stations, Fort Yokon (b') and Churchill (b'').

The thin line in the upper figure (a) is the Δf min of 3 solar side stations and clearly shows the occurrence of (PCA)_p event at 07h on Feb. 10 (indicated by the letter α). The “(PCA)_p event” means the enhanced ionization at the pole (Hakura and Nagai 1964). These curves of Δf min in the polar region show a tendency of gradual increase of PCA till the occurrence of SSC. On the other hand, the mean Δf min at 7 auroral zone stations (b) shows a sudden increase of ionization at about 12h on Feb. 10 (indicated by the letter β). The increase occurred in good time-coincidence with the distinct start of PCA on the riometer records of two auroral zone stations. This phase of PCA is named (PCA)_A in the present analysis.

In a previous publication of this series Nagai (1964) pointed out the simultaneous occurrence of a polar geomagnetic disturbance with the sudden development of PCA in the auroral zone which preceded the onset of SSC at 01:26 on Feb. 11, 1958. Fig. 2 gives a further support to his idea, comparing the storm-time varia-

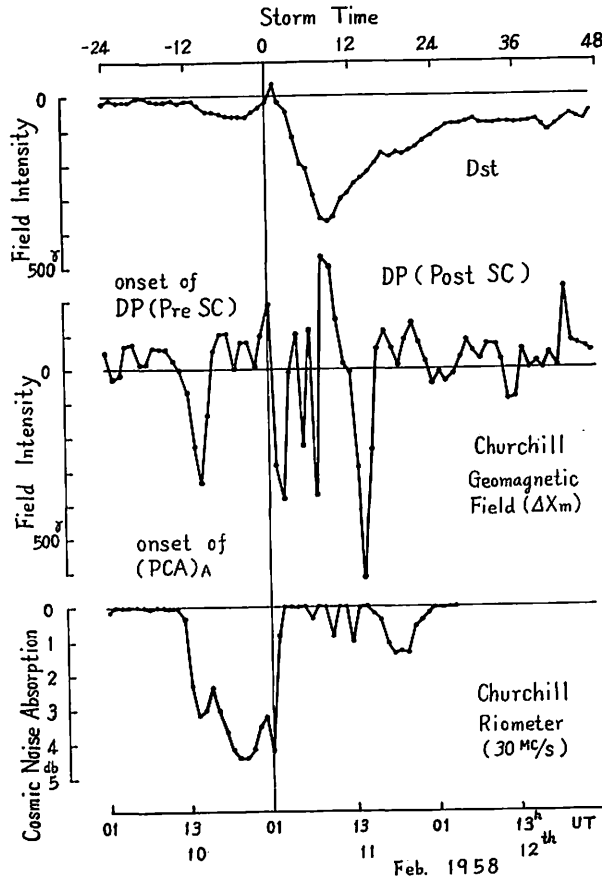


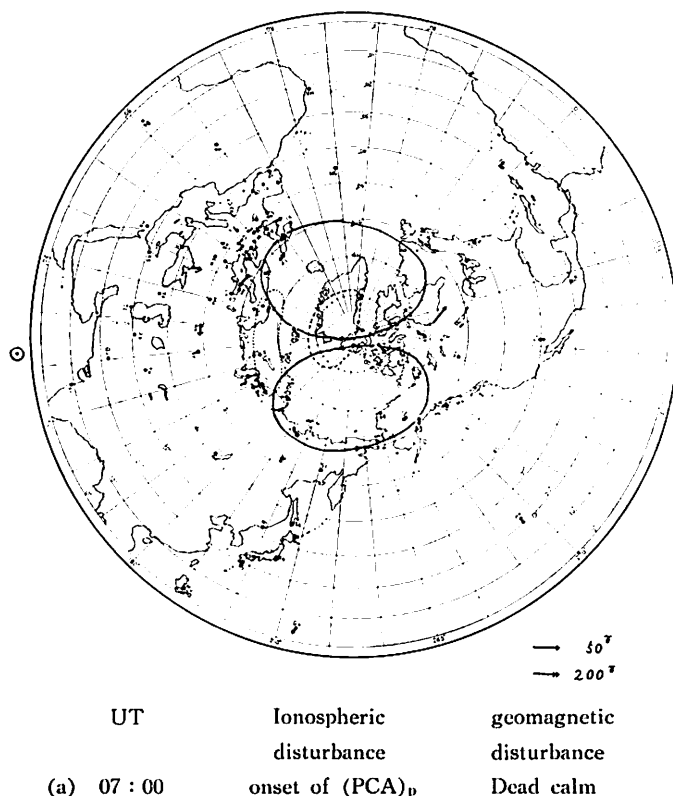
Fig. 2 Storm-time variations of Dst (32.5°), ΔX_m (Churchill), and cosmic noise absorption at Churchill (D. H. Jelly, 1961).

tions of $Dst^{32.5}$ (a) and ΔX_m of the geomagnetic storm, (b) with that of cosmic noise absorption record (c) at Fort Churchill. As indicated by the arrows in the figure, the pre-SC polar disturbance (DP (Pre SC)) started at -13h of the storm time, showing rather surprising time-coincidence with the onset of $(PCA)_A$.

Fukushima (1962 b) showed that, using the K-indices for the IGY period, (a) some geomagnetic agitation takes place almost always in the polar regions when

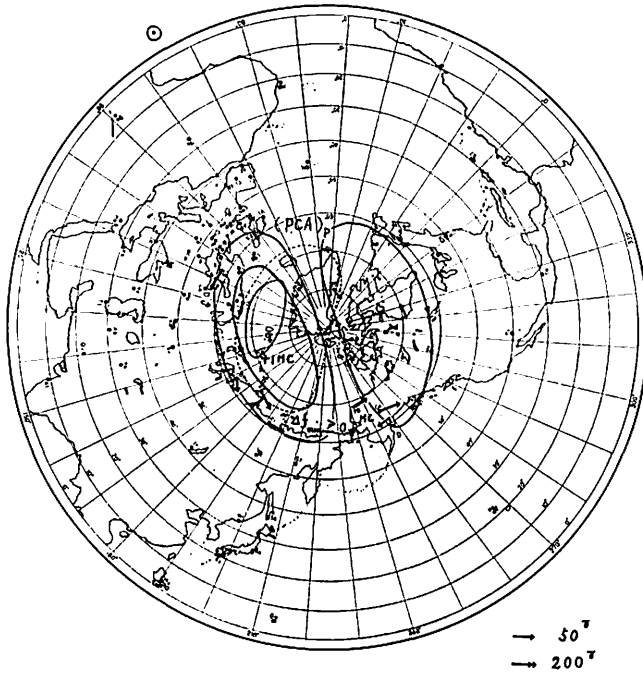
Fig. 3-(a)-(h) Sudden development of PCA in the auroral zone and associated polar magnetic disturbance far before the sudden commencement, drawn on the northern world maps in geomagnetic coordinates.

Enhanced ionization is expressed by the contour of Δf min. The region of complete polar blackouts (B) is hatched. DS-field of geomagnetic storm is expressed by equivalent current system, where the electric current between successive lines is 1×10^5 amp.



the geomagnetic field as a whole is extremely quiet, namely $K_p = O_0$, the disturbance in the sunlit polar cap being definitely larger than those in the dark polar cap, and (b) the polar cap area only is disturbed without the auroral zone enhancement when the K_p value is zero or very small, but the auroral zone disturbances increase and become larger than the simultaneous polar cap disturbances with increase in the K_p value.

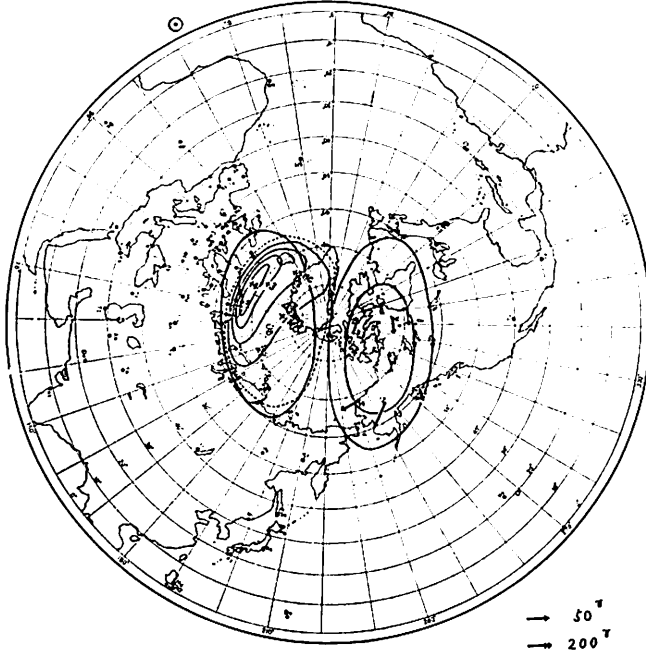
In further investigation, analyzing the IGY geomagnetic data in both Arctic and Antarctic regions, Nagata and Kokubun (1962) found that the geomagnetic daily variation field in the sunlit polar cap on geomagnetically quiet day consists not

(b) 11 : 00 (PCA)_p S_q^p -field

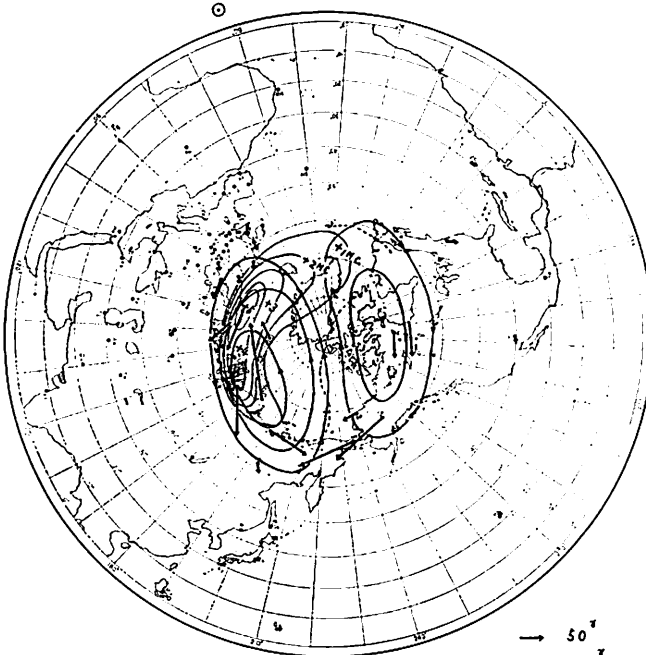
only of the S_q^p -field which is well established in temperate latitudes but also of an additional field, S_q^p -field, the extension of which is limited only within the polar-cap area. The current pattern for the S_q^p -field consists mainly of nearly uniform currents flowing through the central part of the polar cap from 23h to 11h in local geomagnetic time and counter currents flowing through the outerpart of the polar cap, having no auroral zone enhancement. The maximal horizontal geomagnetic force deduced from this current system is about 150 gammas in the sunlit polar cap, but it is reduced to less than one third of its sunlit-value when the polar cap becomes dark.

These results suggest that the S_q^p -field is driven by the solar wind through the lines of geomagnetic force connecting the earth's polar ionosphere with the outer part of the magnetosphere near the boundary wall of the geomagnetic cavity.

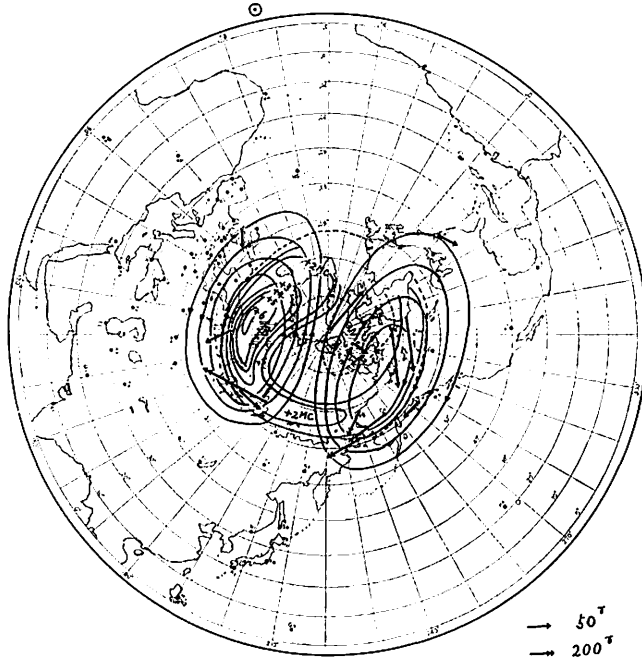
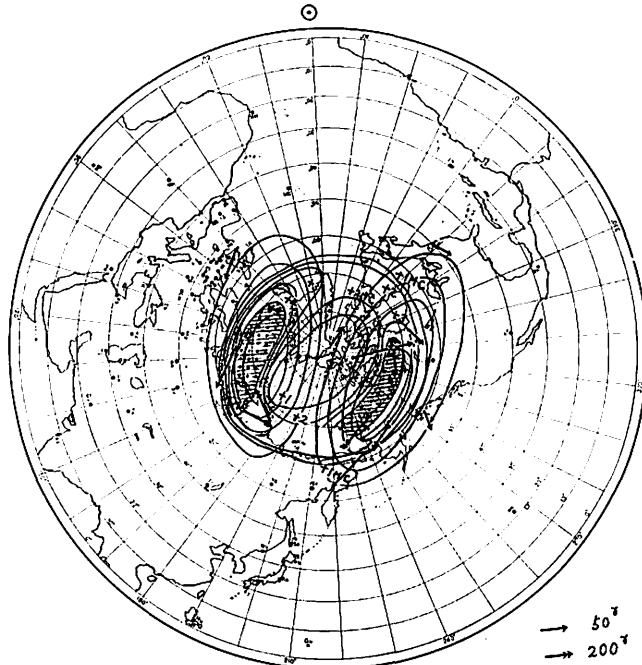
In the present paper, the transient stage from the S_q^p -field to the pre-SC polar disturbance field (DP (Pre-SC)) will be examined in more detail. Fig. 3 (a)-(h) show a series of synoptic patterns of blackouts drawn on the map viewed from the northern geomagnetic pole, with the patterns of equivalent current system which

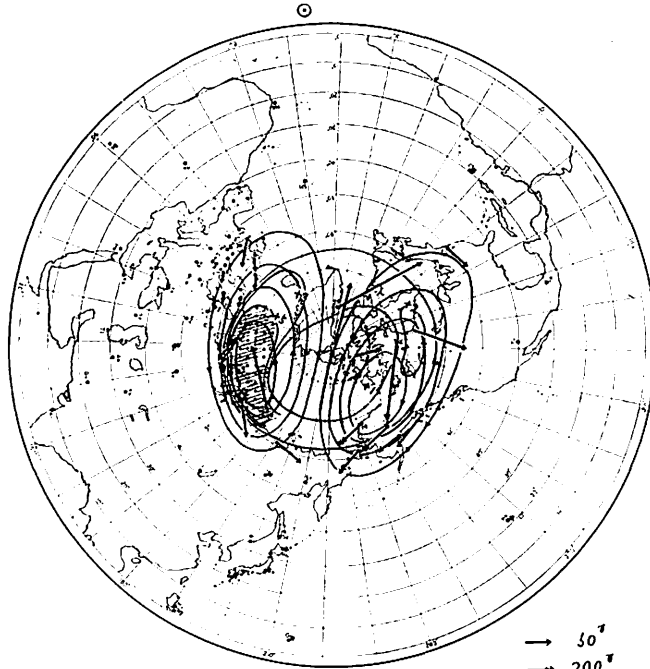


(c) 12 : 00 (PCA)_p develops S_q^p -field

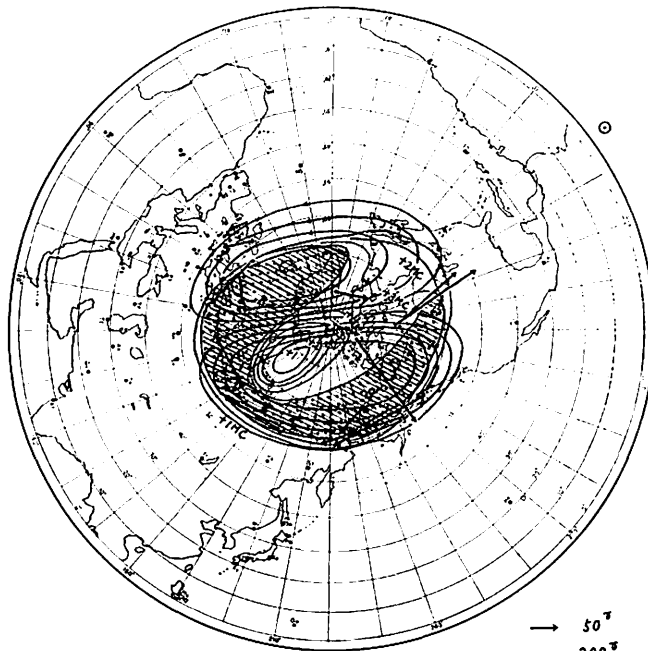


(d) 12 : 30 onset of (PCA) DP (pre SC) starts (transient stage)

(e) 13 : 00 (PCA)_A DP(pre SC)(f) 13 : 30 (PCA)_A DP(pre SC)



(g) 14 : 00 (PCA)_A DP(pre SC)



(h) 18 : 00 (PCA)_A develops DP(pre SC) develops

are responsible for the DS-field of geomagnetic disturbances. The source of data and the method of analysis are explained in Appendix I and II.

(1)-Fig. 3 (a)

A slightly ionized region ((PCA)_p) appeared on the solar side of the polar region at 07h UT on Feb. 10, when the geomagnetic condition was deadly calm. This seems to be the first impact of solar cosmic rays on the earth's polar ionosphere. (stage a)

(2)-Fig. 3 (b)

The region of (PCA)_p was enlarged gradually toward the auroral zone until the occurrence of (PCA)_A. At 11 : 00 on Feb. 10, an example of such an enlarged (PCA)_p event right before the onset of (PCA)_A is shown. Geomagnetic condition was almost quiet.

(3)-Fig. 3 (c)

At 12 : 00 on Feb. 10, the ionization started to increase over the sunlit auroral zone (around Tromsø). However, polar geomagnetic horizontal intensities were still smaller than 50 gammas and strong enhancement of the current in the auroral zone was not yet observed at this stage. Circulations of the equivalent current vectors were clockwise on the morning side and counterclockwise on the evening side. Consequently, it seems that the equivalent current pattern at this stage is essentially the same as the polar cap current system of the S_q^p -field.

(4)-Fig. 3 (d)

At 12 : 30 on Feb. 10, the region of abnormal ionization suddenly began to expand towards the afternoon side. Simultaneously, the horizontal intensities both in the afternoon (Tromsø, Dixon) and the night sides auroral zone stations (College, Big Delta, Kape Wellen) were increased up to about 100 gammas while at the polar cap stations (Thule, Resolute Bay, Godhavn) they were about only 20-30 gammas. The result shows that the transition from the S_q^p -field to the pre-SC polar disturbance (DP (Pre-SC)) field is closely connected with the invasion of PCA-producing solar cosmic rays into the polar ionosphere. Pre-SC disturbance field was intensified with enhanced ionization in the midnight auroral zone, though the intensity of original S_q^p current is greater in the sunlit polar cap than the dark polar cap, and its extension is limited only within the polar-cap area.

(5)-Fig. 3 (e)

At 13 : 00 on Feb. 10, the region on (PCA)_A was elongated to the night side of the auroral zone including Fort Yukon and Churchill, where, at the same time, riometer records indicated a clear onset of cosmic noise absorption (see Fig. 1). Simultaneously, the polar geomagnetic disturbance was intensified in the midnight region

more than in the afternoon side auroral zone. At this stage, horizontal intensities were about 300 gammas at College, and 200 gammas at Dixon. It should be noted that the polar geomagnetic disturbance started at this stage far before the sudden commencement at 01 : 26 on Feb. 11, originating in the region of increased ionization. However, most active Δf min region in the afternoon side around Tromsø ($\Delta f = 6 \text{ MC/s}$) was not coincident with the geomagnetic active region in the midnight auroral zone around College, observed horizontal intensity of about 300 gammas. Although the equivalent current system at this stage is characterized by the enhancement of currents in the auroral zone, it is clear that the pattern of DP (Pre-SC) current system looks very similar to that of S_q^p -field, showing clockwise circulation on the morning side and counterclockwise on the evening side in northern hemisphere. (6)-Fig. 3 (f)

At 13 : 30 on Feb. 10, the ionization continued to increase and complete blackout occurred in the evening side auroral zone around Dixon, and the horizontal intensity at Dixon was about 300 gammas. On the other hand, at College Δf min was only 1 MC/s, and the horizontal intensity was about 400 gammas.

(7)-Fig. 3 (g)

At 14 : 00 on Feb. 10, complete blackout developed in both the morning side and the afternoon side. However, the horizontal intensity of polar disturbance was not so intensified, at Dixon and Point Barrow were both about 300 gammas and at College was 200 gammas, while in the polar region the horizontal intensity at Thule was 160 gammas which was the largest among the disturbance occurred during the pre-SC stage.

(8)-Fig. 3 (h)

At 18 : 00 on Feb. 10, complete blackouts extended over the great part of the auroral zone, while the ionization was gradually intensified in the polar region. At this stage, the geomagnetic disturbance was mostly active in the auroral zone, the horizontal intensity was 400 gammas at Dixon, 350 gammas at College, and about 250 gammas at Tromsø, but at Thule in the polar cap was about only 50 gammas.

In accordance with the development of Δf min, it seems to increase the electron density at the E-region level. Consequently, the currents flowing in the E-layer are also intensified. However, as above mentioned, more detailed analysis shows that the most intensified region of the horizontal current is not necessarily coincident with the maximum ionized region which is indicated by the development of Δf min. The center of the maximum ionized region removes from afternoon side to midnight within about 2 hours. On the other hand most intensified region of the horizontal current removes suddenly from sunlit region to midnight within

only 30min-1 hour.

The centers of the active region of PCA and the horizontal intensities of polar disturbance in the auroral zone are summarized in Table 1.

Table 1. Development of PCA and Geomagnetic Polar Disturbance

			PCA		Geomagnetic disturbance				Remarks	
Fig. 3	Date	Time UT	Max. Δf /min	Center of active region	Horizontal Intensity (γ)				PCA	Geomag. Field
					Thule	Troms ϕ	Dixon	College		
(a)	10 th	07:00	MC/s 0.5	Solar side of Polar region					onset of (PCA) _p	Dead Calm
(b)		11:00	1		25 γ	25 γ	25 γ	25 γ	(PCA) _p	S _q ^p
(c)		12:00	4	Troms ϕ	50	25	—	25	(PCA) _p develops	S _q ^p
(d)		12:30	5	Troms ϕ	25	50	100	100	onset of (PCA) _A	Transi-ent stage
(e)		13:00	6	Troms ϕ	100	50	200	300	(PCA) _A	D P (Pre SC)
(f)		13:30	B	Dixon	125	75	300	400	(PCA) _A	D P (Pre SC)
(g)		14:00	B	Dixon College	160	75	300	200	(PCA) _A	D P (Pre SC)
(h)		18:00	B	Troms ϕ Dixon College	50	225	375	325	(PCA) _A develops	D P (Pre SC) develops

§ 3. Unusual increase of ionization right before the SC1.....(PCA) pre SC1

Right before the sudden commencement, i.e. at 01:00 on Feb.11, the whole polar cap was suffered from complete blackouts (WPCBO). At this stage, an unusual increase of ionization was detected by the cosmic noise absorption measurement (Axford and Reid, 1962). The remarkable enhancement is seen at the stage γ of riometer traces of Fort Yukon, Alaska and Churchill, Canada, in Fig.1-(b') and (b''). The universal time change of absorption (Δf min) in the polar region also shows the pre-SC enhancement of PCA (PCA) pre SC1) in Fig. 1-(a).

They interpreted the effect in terms of compression of the particles between two shockwaves in the interplanetary medium. One of these shock waves is formed in front of the advancing solar gas cloud and propagates through the interplanetary

space supersonically and produces the sudden commencement of a geomagnetic storm at its attainment to the earth, whereas the other is a standing shockwave set up by the motion of the solar wind past the earth's magnetosphere. During a similar event on September 30, 1961, the equipment on board the satellite Explorer XII and Injun I confirmed their prediction that the enhanced absorption is due to an increase in the low-energy protons whose energy is less than 100 Mev.

In the present section, the latitudinal extent of the pre-SC enhancement will be discussed in some detail. The middle part of Fig. 4 shows the timevariation of the boundaries of PCA, obtained on the analysis of Δf min and riometer records at 19 ionospheric stations. The thick lines in the figure represent the boundary of the blackout region, whereas the thin lines are the iso- Δf min curves in step 1.0 MC/s. In the upper part of the figure, the Churchillriometer is again reproduced to show the time change of PCA intensity inside the blackout region.

During the pre-SC enhancement of PCA (stage γ), the upper boundary of the absorption remarkably shifted towards the northern pole, whereas the lower boundary remained almost unchanged and stayed around the latitude of Anchorage, Alaska (+60.5° corrected g.m. lat.). The pattern of WPCBO (the whole polar cap blackout) (shown in Fig. 5-a (left)) is due to the (PCA) pre SCI around the pole. The pre-

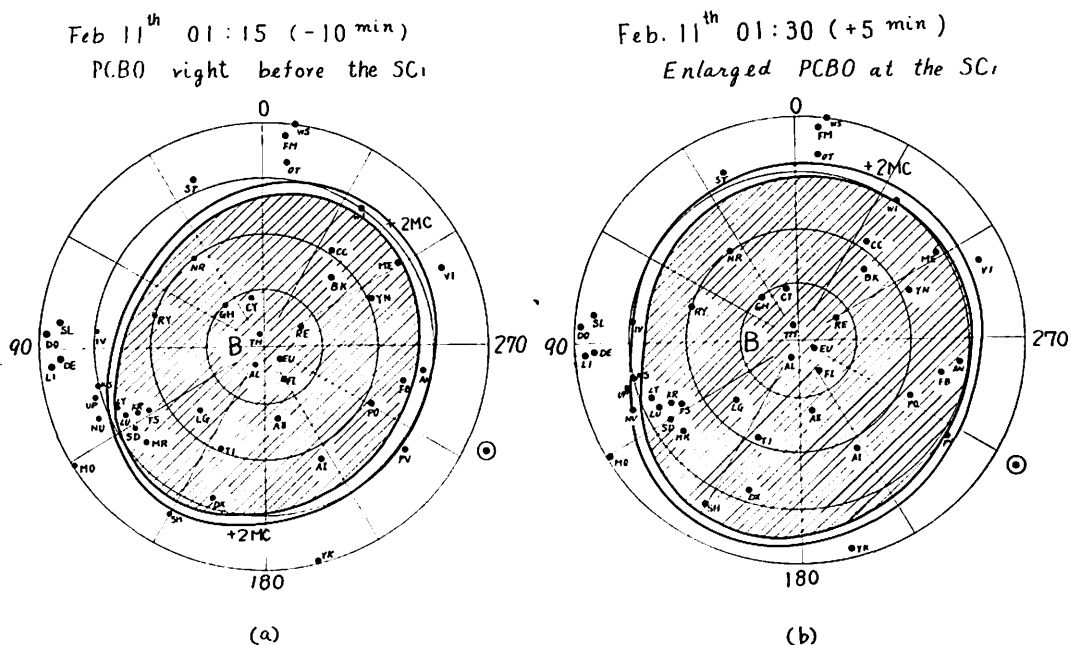


Fig. 5 (a) and (b) : PCBO right before and after the SCI (01 : 26 on Feb. 11).

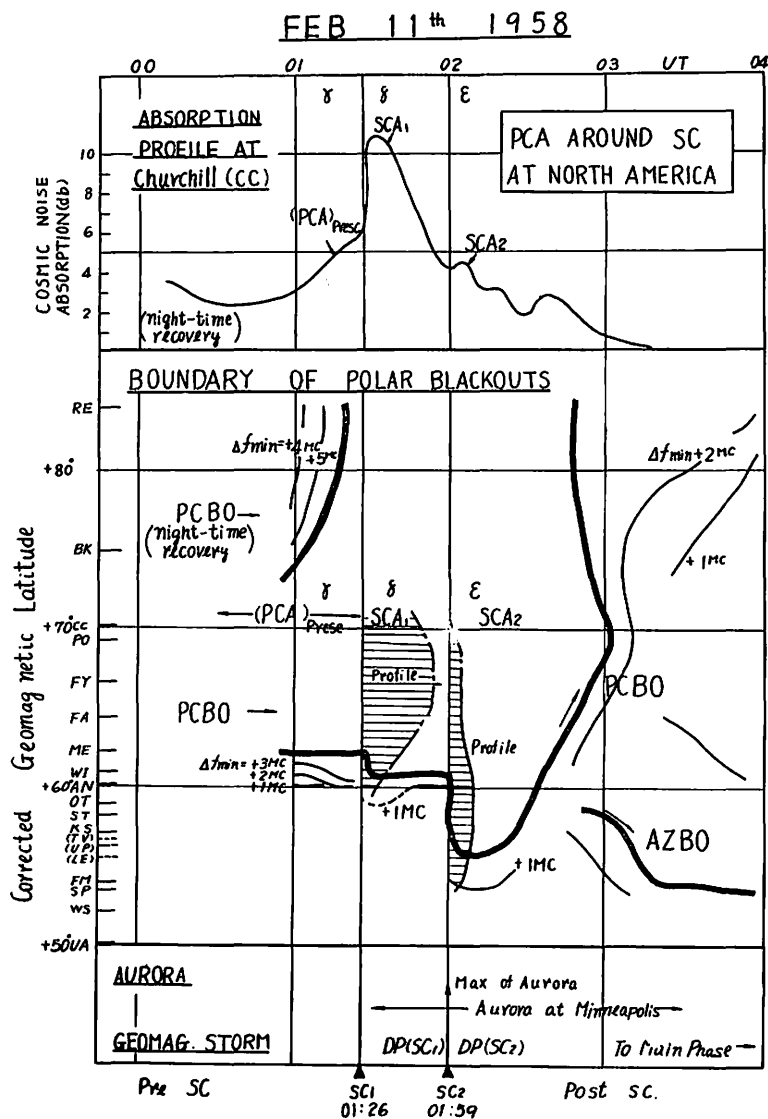


Fig. 4 Outstanding changes of PCA around the 2-stepped sudden comments of Feb. 11, 1958 (Successive occurrence of (PCA) pre-SC1, SCA1, SCA2, and deformed PCBO). Absorption profile at Churchill : Cosmic noise absorption observed by riometer at 30.0 MC/s (after Axford and Reid, 1962). Boundary of polar blackouts : Thick lines show the boundary of complete blackouts, while thin lines are contours of iso Δf_{\min} Ionization profiles at SC1 and SC2 are obtained by the standardized Δf_{\min} and cosmic noise absorptions at 19 stations. Aurora : Observation at Mineapolis at 56.8 corr. g. m. lat.) after Winckler, et al., 1959)

sent analysis thus, clarified the fact that the pre-SC invasion of accelerated interplanetary particles took place over the whole polar cap above 60° in corrected geomagnetic latitude. The result shows a difference from the PCA events on May 8, 1960, and September 30, 1961, where the pre-SC increase of absorptions was not evident at high-latitude stations, whereas a clear increase occurred at the auroral-zone stations, suggesting that rather broad differed impact zone exists for the accelerated protons in the auroral-zone latitudes (Axford and Reid, 1963). However, it seems quite possible that the impact zone broadens with the increasing intensity of accelerated particles of lower energies. The pre-SC enhancement of February event was the severest among three examples discussed here. The time change of upper boundary of PCBO of this event (Fig. 4, stage γ) actually shows the broadening of the impact zone in coincidence with the increasing absorption at Churchill riometer.

**§ 4. Outstanding geomagnetic and ionospheric disturbances
associated with two successive sudden commencements
.....SCA1 and SCA2; DP (SC 1) and DP (SC 2)**

The appearance of the earth storms associated with two successive sudden commencements on Feb. 11 was really spectacular. To understand a variety of violent terrestrial disturbances, the world-wide changes in the magnetograms are reviewed. In Fig. 6-(a), longitudinal variations of the geomagnetic disturbance are displayed in terms of horizontal intensities observed at four middlelatitude stations situated at equal longitudinal intervals (Kakioka, 206.1° g.m. longitude; Tucson, 312.2° ; San Juan, 3.2° ; Tashkent, 143.8°) Fig. 6-(b) and (c) give the latitudinal changes that appeared in both the North American and the European regions, where the horizontal components of geomagnetic intensities at several stations are arranged in the order of their geomagnetic latitudes.

In all these magnetograms, two sharp increases are seen at low latitude stations at 01:26 and 01:59 respectively on Feb. 11 to indicate the occurrence of successive sudden commencements of the geomagnetic storm (SC1 and SC2). Following the sudden commencements, violent polar geomagnetic disturbances were observed in all the magnetograms displaying remarkable diurnal variations (DP(SC1) and DP(SC2)). (Hakura and Nagai 1964).

Fukushima and Abe (1958), in their analysis of 7 Japanese magnetograms, examined the latitudinal dependence of DP (SC1) and predicted that the disturbance must be of polar origin.

In the previous paper, Nagai (1964) has reported that, using the geomagnetic

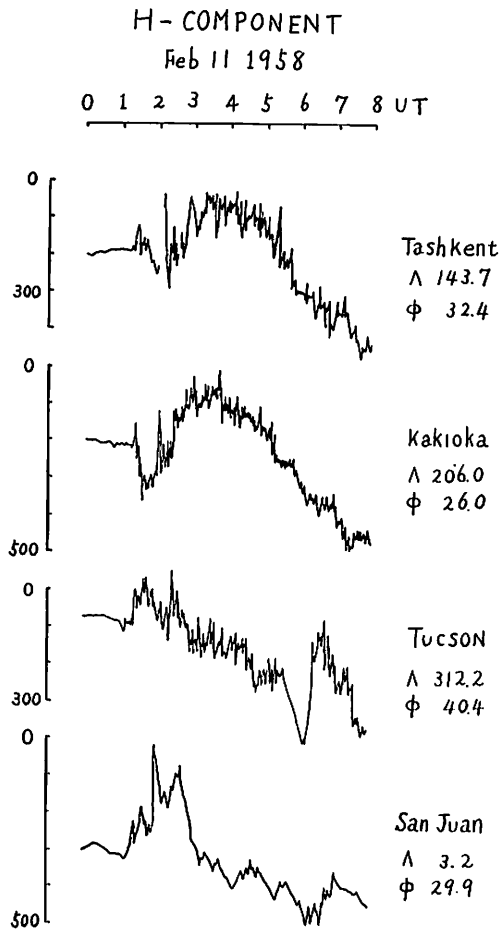


Fig. 6 Remarkable variations of geomagnetic field in the earlier part of the Feb. 11, 1958, event, expressed by the horizontal components of various stations.

Fig. 6-(a) : Local time variation in the middle latitude.

northern hemisphere, the most active DS field happened suddenly one hour after the SC(+ 1 hr) almost all over the auroral zone and the polar cap. Such DS field reached to -1400 gammas at Troms ϕ (67.1° g.m. latitude) and -700 gammas at Lovö (58.1°), but at Rude-Skov (55.8°) it was only -50 gammas. There is a clear boundary between Lovö and Rude-Skov, and which coincides with that of the blackouts. The polar current of the DS field at +1 hr flows parallel with the meridian of about 15h-17h at Thule and Godhavn. These results are the outstanding characteristics of this storm which had not been observed in the other storms occurred during the IGY. In

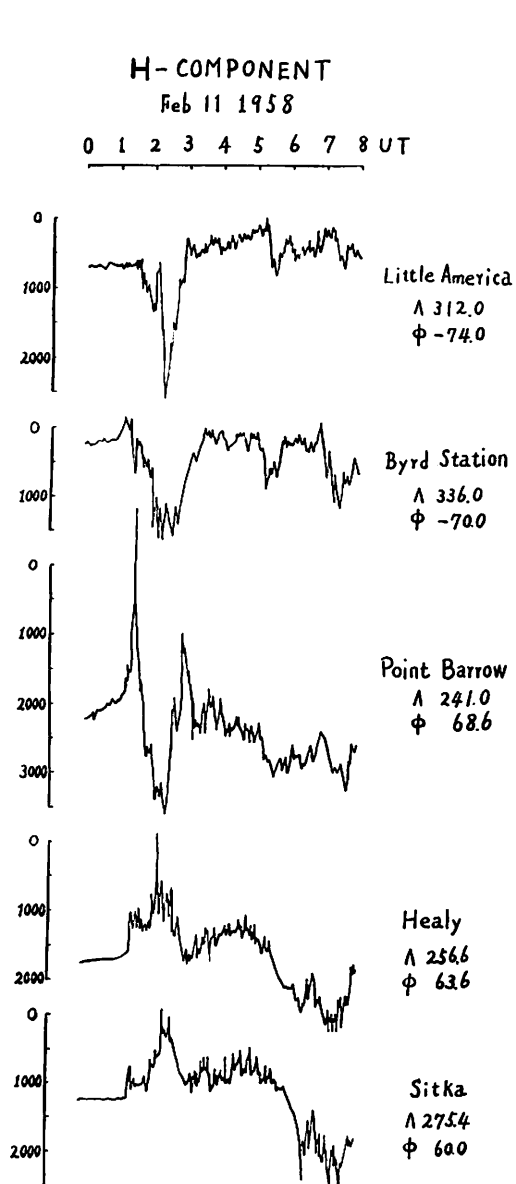


Fig. 6-(b) : Latitudinal change in North American region.

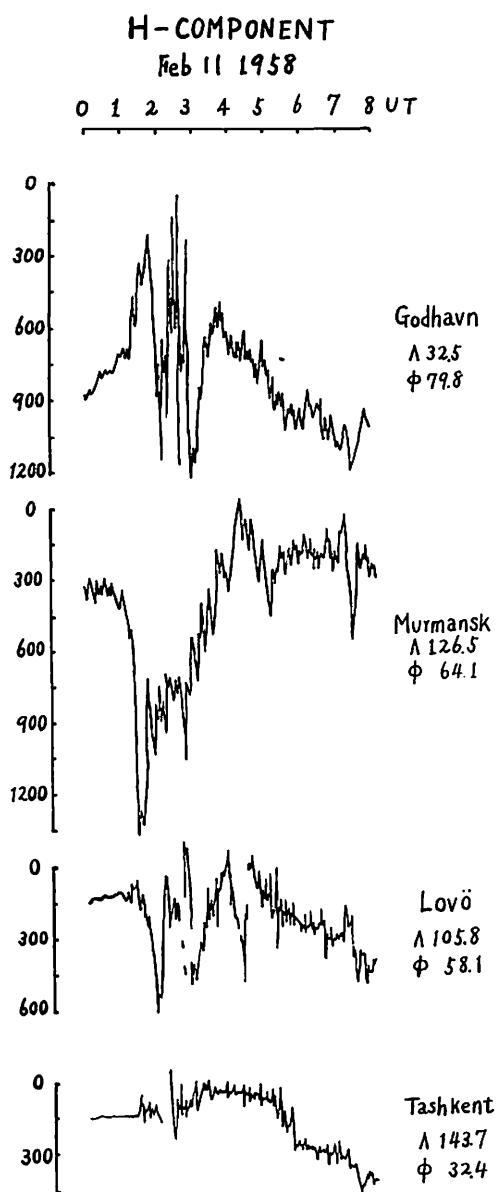


Fig. 6-(c) : Latitudinal change in European region.

general, DS field develops gradually in accordance with the development of Dst field. Obayashi and Jacobs (1957) have shown that a systematic change in the shape of SC's exists with geographic longitude; that is, the amplitude of SC's is strongly dependent on the local time of their occurrence, tending to depress or reverse in the

horizontal component in the forenoon hemisphere, while it is enhanced in the afternoon hemisphere. Though the shape of SC's is more or less the same for any station in low latitudes, it is thus clear that the local time effect is predominant in the polar regions. Oguti (1961) has found in the records of the three cases which obtained during the IGC, when the simultaneous observations of magnetic field and auroral luminosity at syowa Station was carried out, that there is a strong evidence for the geomagnetic SSC* to be related directly with auroral activity. The coincidence of negative kick in SSC* with the peak of the luminosity curve in zenital aurora is found to be almost complete. This fact seems to suggest that SSC* has its origin in the low ionosphere as has been already pointed out by Nagata and Abe (1965).

The present analysis has revealed somewhat detailed appearance of two stepped polar geomagnetic disturbances.

The equivalent current systems derived from above mentioned violent magnetic variations SC1 and SC2 which occurred at 01 : 26 and 01 : 59 Feb. 11 respectively are drawn in Fig. 7-(a) and (b). The current systems indicate that the DS field

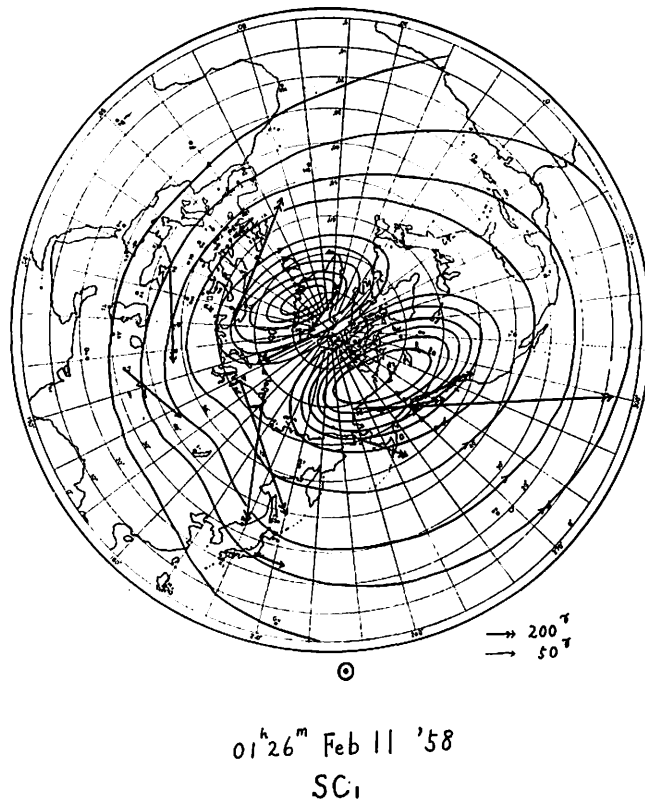


Fig. 7 (a) : Equivalent current-system of SC1 at 01 : 26 on Feb. 11, 1958.

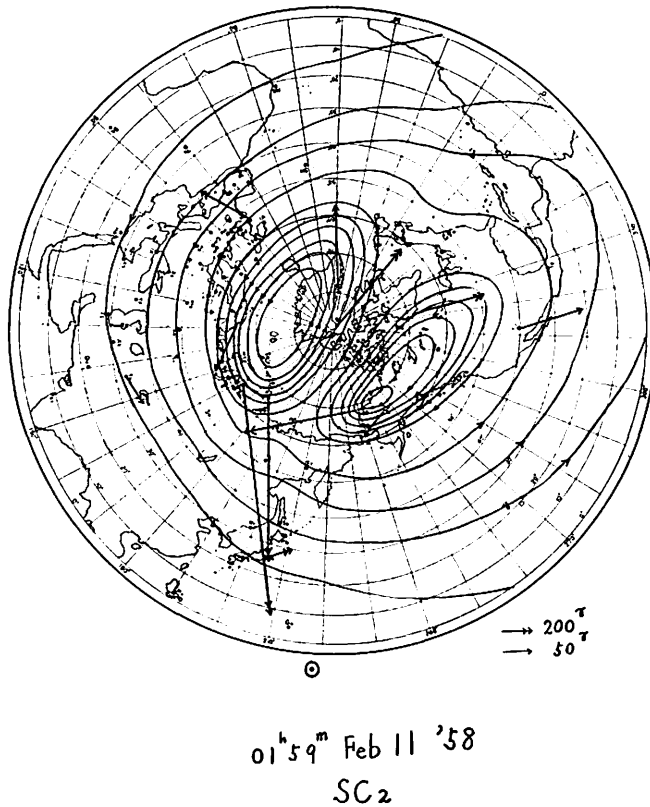


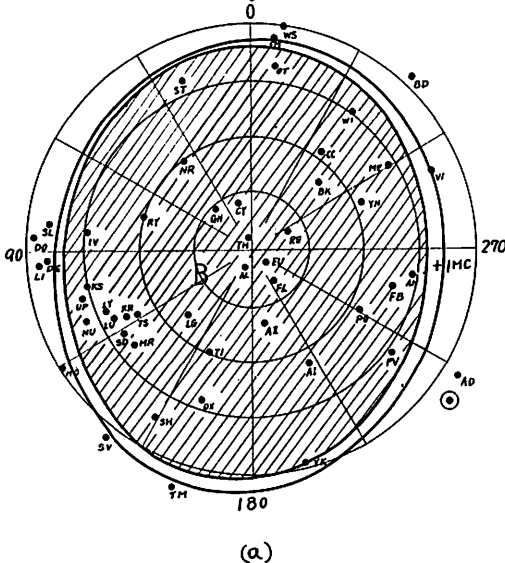
Fig. 7 (b) : Equivalent current-system of SC2 at 01 : 59 on Feb. 11, 1958 predominates in Auroral zone rather than in polar regions, while the Dst field prevails in low latitudes. The pattern of current system of SC1 is quite similar to that obtained by many workers, although the currents are more intense than others, and considerably wide spread almost over the entire auroral zone. In the outer auroral zone, currents in both the D_{st}^c and D_{st}^c -parts flow towards the east in the afternoon. In the forenoon, however, the D_{st}^c current flows westwards against the eastwards D_{st}^c current. The equivalent currents in the central part of the polar cap are directed from 20h towards 08h in local geomagnetic time. On the other hand, the straight current of SC2 flows in the opposit direction from 09h towards 21h in local geomagnetic time. It is very interesting that above result agrees with the direction of SSC*obtained by Nagata and Abe (1955).

In accord with the geomagnetic disturbances, the region of polar cap black-outs also showed remarkable expansions. The Pattern of enhanced ionization at 01 : 30 shown in Fig.5-(b) (right) suggests that the first expansion occurred within at

most 5 minutes after the SC1. Detailed patterns of the boundary change have been obtained on the analysis of ionospheric data at 19 polar stations and are shown in the middle part of Fig. 4. Immediately after the SC1, the lower boundary of the enhanced ionization suddenly shifted to the south by a few degrees of corrected geomagnetic latitude.

The profile of ionization intensity may be estimated at the analysis of the standardized cosmic noise absorptions and Δf min's. As shown by the hatched region in Fig. 4 (indicated by the letter δ), the region of increased ionization right after the SC1 is confined within some extended auroral zone including Churchill and Anchorage. The profile may be identified with that at the SCA (Sudden Commencement Absorption) which is now widely recognized as the absorption associated with complex types of sudden commencements (Brown, et al., 1961; Ortner, et al., 1961; Matsushita, 1961). Thus the present ionization is called SCA1. The origin of sudden commencement absorption (SCA1) is considered to be the dumping electrons from a part of Van Allen belts which were compressed by the shock wave responsible for the SC1. Indeed, the bright aurora was visually observed simultaneously with the SC1 even in the subauroral zone of the North American region, showing the invasion of electron beams into the lower ionosphere (Winckler, et al., 1959).

Feb. 11th 02:15 (+50 min)
Further Enlarged PCBO at the SC2



Feb. 11th 02:45 (+80 min)
Reduced and Deformed PCBO

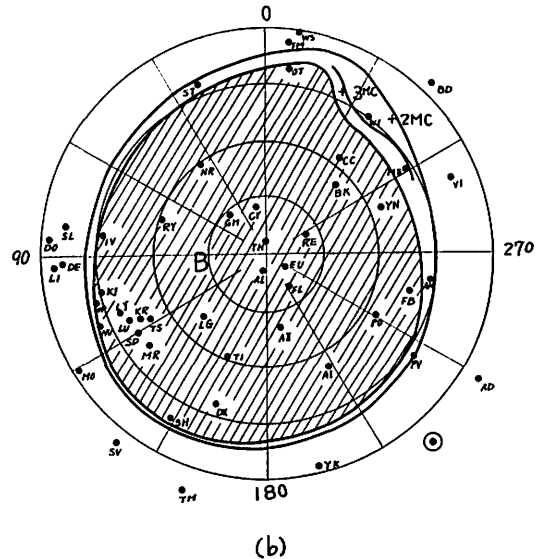


Fig. 8 (a) and (b) : Change of PCBO after the SC2 (01:59 on Feb. 11).

Axford and Reid (1962) identified the enhanced absorption at this stage with the continuation of (PCA) pre SC1. It is very likely that a part of the enhanced ionization associated with SC2 was produced by the particles stored in a space between two shock-waves which were responsible for SC1 and SC2. Such part may be called (PCA) pre SC2.

A more remarkable southward shifting of PCA boundary was observed after the SC2, as shown in Fig. 4 (stage ϵ) ; at its maximum phase, the border of enhanced ionization attained even to Sampson, Canada. Fig. 8-(a) (left) shows the maximum phase of the expanded PCBO region which appeared at 02:15 UT on Feb. 11. The absorption profile at this stage is also given in Fig. 4 ; as shown by the hatched region (indicated by ϵ), enhanced ionization covered the wide range between Churchill and Sampson ($+70^\circ \sim 53.6^\circ$ in corrected geomagnetic latitudes $\equiv 8.5 R_E \sim 2.8 R_E$ equatorial distances of the corresponding geomagnetic field). The sudden commencement absorption (SCA2) might be connected to the second attack of shock wave to the earth whose influence reached unexpectedly inner region of Van Allen belt, squeezing out the trapped electrons into the subauroral ionosphere. It is tempting to note that the intense and dynamic aurora of higher latitude were observed even at Minneapolis ($+56.8$ c. g. m. l.) at this stage of disturbance (Winckler, et al., 1959).

Several years ago, Obayashi (1958) estimated the change of equivalent geocavity boundary size, on the analysis of the changing period of geomagnetic pulsations in the course of the present geomagnetic storm. Though the change is not of a monotonic curve as he drew, the original values show a very good coincidence with the boundary change of PCBO shown in Fig. 4, when we transform the cavity boundary (R_C) to the geomagnetic latitude (ϕ), using the formular: $R_C = R_E \sec^2 \phi$. The result gives further support to the idea that the influence of two-stepped shock waves reached the inner region of the earth's atmosphere far beyond the ordinary cavity boundary at the time of SC's on Feb. 11, reducing the period of pulsation through their excitement of inner geomagnetic field, and squeezing out the particles stored in the region.

§ 5. Directions of the straight currents in the central part of the polar cap.

Equivalent current-systems of polar geomagnetic disturbances, such as SD or DS, geomagnetic bay (B), the polar part of SSC (D_i^c) and SSC* fields, have been studied by many workers. Some typical characteristics of these current systems in the polar regions are summarized in Table II. On an average, the currents in the

Table II. Intensity and Direction of Polar Current-Systems

Author	Current system	Intensity (10 ⁴ A)	Direction
Chapman (1935)	SD	45	12h
Vestine (1947)	DS	180	8
Nagata, Fukushima (1952)	DS	32	9
Nagata, Kokubun (1961)	DS(South)	60	9
Vestine, Silsbee (1942)	Bay	50	8
Obayashi (1956)	D _s ^c	15	9
Nagata, Abe (1955)	SSC*	7	22
Vestine (1947)	(Sq)	5	10
Nagata, Kokubun (1962)	S _q ^p	16-14	11

central part of the polar cap are directed from 22h towards 10h in local geomagnetic time in S_q^p, DS, B and D_s^c, while those of SSC* are just in the opposite direction.

However, it is also known that these directions of the straight currents in the central part of the polar cap display considerable changes in the course of individual polar geomagnetic disturbances. In the present study, the patterns of the directional changes are examined in each stage of the severe magnetic storm ; pre-SC phase, initial phase, main phase and last phase.

Fig. 9 shows the hourly values of Dst₀, and the intensity of horizontal vectors $\sqrt{\Delta X^2 m^2 + \Delta Y^2 m^2}$, and the directions of the straight currents at Thule during 2 days from -24hr to +24hr (storm time). The length of the current arrow shows an intensity of horizontal vector $\sqrt{\Delta X^2 m^2 + \Delta Y^2 m^2}$. And the direction of the current arrow shows a local geomagnetic time which indicates the midnight meridian in north direction.

During the pre-SC polar disturbance (-12hr ~ -1hr), the directions of the straight currents indicated 08h ~ 13h. In the initial phase, at 0 hr and +1 hr of storm time, the directions of the straight currents indicated 10h and exceptionally abnormal direction 16h as already reported in the previous paper (Nagai, 1964). During the developing stage of Dst field (+3hr ~ +7hr), the directions of the straight currents indicated 07h ~ 08h which was mostly inclined towards morning side. On the other hand, during the recovering stage of Dst field (+10hr ~ +18hr), the directions of the straight currents gradually shift towards afternoon side, indicated 11h ~ 13h in local geomagnetic time.

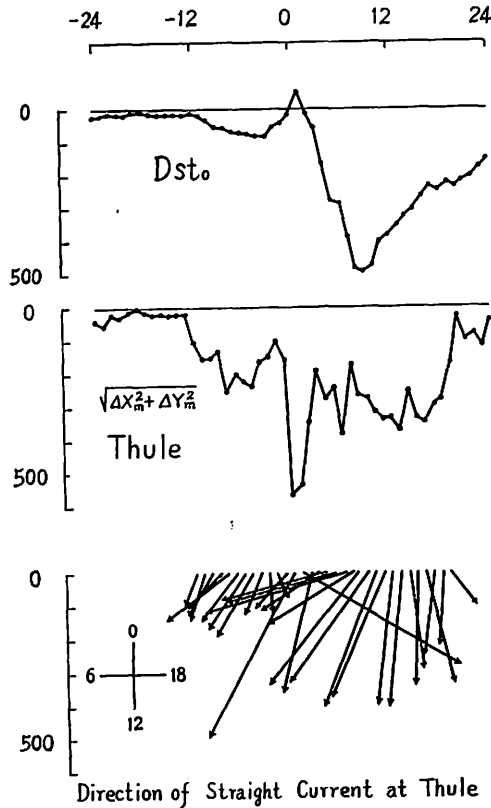


Fig. 9 Directions of the straight currents in the central part of the polar cap.

- (a) Storm-time variation of Dst_0
- (b) Intensities of horizontal vector at Thule.
- (c) Directions of the straight currents in local geomagnetic time (The length of the current arrow shows an intensity of horizontal vector)

Above results obviously show that the directions of the straight currents do not depend on the intensity of the horizontal vector at Thule, alternatively depend on the developing and recovering stages of the Dst field.

§ 6. Conclusions

In the present paper, an attempt is made to reexamine several interesting phenomena related to polar geomagnetic disturbances and PCA Events on February 11, 1958. The important experimental results obtained here are described with some speculations as follows :

(1) A sudden development of PCA started in the sunlit auroral zone at 12 : 00 on Feb. 10. The enhanced ionization $(PCA)_A$ encircled the whole auroral zone within an hour or two, and then developed gradually till the blackout condition was attained over the whole polar cap right before the sudden commencement at 01 : 26 on Feb. 11.

A geomagnetic disturbance DP (Pre SC) was observed over the polar region, simultaneously with the occurrence of $(PCA)_A$, for preceding the SSC on Feb. 11. Because of the absence of usual Dst-part, the DP (Pre SC) is considered to be a special disturbance whose origin is connected with the invasion of PCA-producing solar cosmic rays into the polar ionosphere.

At 12 : 30, transient stage from the S_q^p field to the DP (Pre SC) was found DP (Pre SC) field was intensified with enhanced ionization at the midnight in auroral zone. The current pattern of the S_q^p -field resembles very much with that of the DP (Pre SC) field, though the former is limited within the polar-cap area and there is no auroral zone enhancement of the currents.

(2) An unusual increase of ionization occurred right before the onset of the SSC over the whole polar cap ((PCA) Pre SC). Axford-Reid model (1963) of 2 shock-fronts acceleration of interplanetary particles may be accepted as its origin. Some progressive pattern of the impact zone for the particles was obtained in the analysis of a number of ionospheric data. The upper boundary remarkably shifted towards the geomagnetic pole with the increasing flux density of energetic particles, while the lower boundary remained almost unchanged at the latitude of about 60° throughout the course of the event.

(3) The equivalent current systems of the two successive sudden commencements at 01 : 26 and 01 : 59 on Feb. 11 (SC1 and SC2) were obtained. The pattern of current system of SC1 is quite similar to the formerly obtained by many workers, though the currents are more intense than others and spread considerably wider covering almost over the entire auroral zone. In the outer auroral zone, currents in both the D_{ii}^c and D_{is}^c -parts flow towards the east in the afternoon. In the forenoon, however, the D_s^c current flows westwards against the eastwards D_{ii}^c current. The equivalent currents in the central part of the polar cap are directed from 20h towards 08h local geomagnetic time. On the other hand, the straight currents of SC2 flow in the opposite direction from 09h towards 21h in local geomagnetic time. This result agrees with the direction of SSC* obtained by Nagata and other's.

In accord with the geomagnetic disturbances, the region of polar cap blackouts also showed two-stepped expansions. By the use of corrected geomagnetic coordinates, the transient boundary changes in blackout region and the ionization

profiles were clarified in their details. Consequently, the additional twosteped ionizations were identified with a kind of the sudden commencement absorptions (SCA1 and SCA2). The origin of SCA's is considered to be the dumping electrons squeezed out from Van Allen belt by the influence of advancing shock waves responsible for the SC's. The speculation is supported by the simultaneous appearance of violent aurora in the sub-auroral zone.

Changes of geo-cavity boundary estimated by obayashi (1958) on the analysis of geomagnetic pulsation periods show a nice coincidence with the boundary changes of PCBO obtained here.

(4) The directions of the straight currents in the central part of the polar cap were examined using the hourly values at Thule during 2 days from -24hr to $+24\text{hr}$ at the storm time. During pre-SC polar disturbance ($-12\text{hr} \sim -1\text{hr}$), the directions of the straight currents indicated $08\text{h} \sim 13\text{h}$. And during the developing stage of Dst-field ($+3\text{hr} \sim +7\text{hr}$), the directions of the straight currents indicated $07\text{h} \sim 08\text{h}$ which was mostly inclined towards morning side. On the other hand, during the recovering stage of Dst field ($+10\text{hr} \sim +18\text{hr}$), the directions of the straight currents gradually delayed towards afternoon side, indicating $11\text{h} \sim 13\text{h}$ in local geomagnetic time.

Consequently, it is obvious that the directions of the straight currents do not depend on the intensity of the horizontal vector at Thule, alternatively depend on the developing and recovering of the Dst field.

Acknowledgments

In concluding, the authors wish to express their thanks to Dr. T. Yoshimatsu, Director of Kakioka Magnetic Observatory and to Dr. H. Uyeda, Director of the Radio Research Laboratories, for their interest in the present study.

The authour are also grateful to Dr. T. Yonezawa, the Radio Research Laboratories, for his discussions and interest in the present study.

The author's cordial thanks are due to Prof. T. Obayashi of kyoto University to Dr. K. Yanagihara, Kakioka Magnetic Observatory, and to Dr. Sinno, Hiraiso Radio Wave Observatory, the Radio Research Laboratories, for their valuable discussions bestowed on the subject.

References

- (1) Akasofu, S.-I. and S. Chapman, Large-scale auroral motions and polar magnetic disturbances-III. The aurora and magnetic storm of 11 February 1958, J. A. T. P., **24**,

- 785 (1962).
- (2) Axford, W. I. and G. C. Reid. Polar cap absorption and the magnetic storm of Feb. 11, 1958, *J.G.R.*, **67**, 1962 (1962).
 - (3) Axford, W.I. and G.C Reid, Increases in intensity of solar cosmic rays before sudden commencements of geomagnetic storms, *J.G.R.*, **68**, 1793 (1963).
 - (4) Brown, R.R., T.R. Hartz, B. Landmark, H. Leinbach, and J. Ortner, Large scaled electron bombardment of the atmosphere at the sudden commencement of a geomagnetic storm, *J.G.R.*, **66**, 1035 (1961).
 - (5) Fukushima, N. and S. Abe, The initial phase of the magnetic storm on Feb. 11, 1958, *Rep. Ionos. Res. Japan*, **12**, 44 (1958).
 - (6) Fukushima, N., Gross character of geomagnetic disturbance during the International Geophysical Year and the Second Polar Year and the Second Polar Year, *Rep. Ionos. Res. Japan*, **16**, 37, (1962).
 - (7) Hakura, Y. and Y. Takenoshita, On the short wave transmission disturbance of Feb. 11, 1958, *Rep. Ionos. Res. Japan*, **12**, 10 (1958).
 - (8) Hakura, Y., Y. Takenoshita and T. Otsuki, Polar blackouts associated with severe geomagnetic storm on Sept. 13, 1957, and Feb. 11, 1958 *Rep. Ionos. Res. Japan*, **12**, 459 (1958).
 - (9) Hakura, Y. and T. Goh, Pre-SC polar cap ionospheric blackout and type IV solar radio outburst, *J. Radio Res. Lab.*, **6**, 635 (1959).
 - (10) Hakura, Y., Development of ionospheric and geomagnetic storms caused by solar corpuscular emissions-I. polar cap blackout and auroral zone blackout, *Rep. Ionos. Space Res. Japan*, **15**, 1 (1961-a).
 - (11) Hakura, Y., M. Nagai and Y. Sano, Development of ionospheric and geomagnetic storms caused by solar corpuscular emissions-II. Polar blackouts, storm Es, and geomagnetic storms, *Rep. Ionos. Space Res. Japan*, **15**, 14 (1961).
 - (12) Hakura, Y., Some statistics on the solar cosmic rays produced by solar eruptions associated with type IV outbursts, *Proc. 12th Alaskan Sci. Conf.* (1961-b).
 - (13) Hakura, Y., and M. Nagai, Synthetic study of severe solar-terrestrial disturbances on February 9-12, 1958, *J. Radio Res. Lab.*, **11**, 197 (1964).
 - (14) Hakura, Y., Patterns of polar cap blackout drawn in a geomagnetic coordinate corrected for the higher terms of spherical harmonic development, *J. Radio Res. Lab.*, **11**, No. 57, to be published (1964).
 - (15) Hultqvist, B., J. Aarons, and J. Ortner, Effects of the solar flare of July 7 1958 observed at Kiruna Geophysical Observatory, Sweden, *Tellus*, **11**, 319 (1959).
 - (16) Huru-hata, M., Aurora and airglow observations on Feb. 11, 1958, *Rep. Ionos. Res. Japan*, **12**, 40 (1958).
 - (17) Matsushita, S., Increase of ionization associated with geomagnetic sudden commencements, *J.G.R.*, **66**, 3958 (1961).
 - (18) Nagai, M., On the magnetic storm on February 11, 1958, *Memo. Kakioka Mag. Obs.*, **2**, 39 (1964).
 - (19) Nagata T., and S. Abe, Note on the distribution of SC* in high latitudes *Rep.*

- Ionos. Res. Japan, **9**, 39 (1955).
- (20) Nagata T., and S. Kokubun, An additional geomagnetic daily variation field (S_q^p -field) in the polar region on geomagnetically quiet days, Res. Ionos. Rep. Japan, **16**, 256 (1962-b).
 - (21) Obayashi, T. and J.A. Jacobs, Sudden commencements of geomagnetic storms and atmospheric dynamo action, J.G.R., **62**, 589 (1957).
 - (22) Obayashi, T., Geomagnetic storms and earth's outer atmosphere, Rep. Ionos. Res. Japan, **12**, 301 (1958).
 - (23) Obayashi, T. and Y. Hakura, Enhanced ionization in the polar ionosphere caused by solar corpuscular emissions, Rep. Ionos. Space Res. Japan, **14**, 1 (1960-a).
 - (24) Obayashi, T. and Y. Hakura, Solar corpuscular radiation and polar ionospheric disturbances, J.G.R., **65**, 3131 (1960-b).
 - (25) Obayashi, T. and Y. Hakura, Propagation of solar cosmic rays through interplanetary magnetic field, J.G.R., **65**, 3143 (1960-c).
 - (26) Oguchi, T. and T. Nagata, Inter-relations among the upper atmosphere disturbance phenomena in the auroral zone, Rep. Ionos. Res. Japan, **15**, 31 (1961).
 - (27) Ortner, J., H. Leinbach and M. Sugiura, The geomagnetic storm effect on polar cap absorption, Arkiv. Geophys., **3**, 429 (1961).
 - (28) Ortner, J., B. Hultqvist, R.R. Brown, T.R. Hartz, O. Holt, B. Landmark, J. L. Hook and H. Leinbach Cosmic noise absorption accompanying geomagnetic storm sudden commencements, J.G.R. **67**, 4169, (1962).
 - (29) Sinno, K., On the great solar flare which started at 21h 09m February 9th, 1958, as the likely source of geomagnetic storm, February 11th, Rep. Ionos. Res. Japan, **12**, 6, (1958).
 - (30) Sinno, K., Some characteristics on solar corpuscular radiations which excite abnormal ionization in the polar upper atmosphere, J. Radio Res. Lab. Japan, **8**, 17 (1961).
 - (31) Winckler, J.R., L. Peterson, R. Hoffman, and R. Arnoldy, Auroral X-rays, cosmic rays, and related phenomena during the storm of Feb. 10-11, 1958, J.G.R., **64**, 597 (1959).

APPENDIX I Data used in present paper

(i) Ionospheric sounding data

In the present analysis we used the vertical ionospheric sounding data at 126 stations (89 in the northern and 37 in the southern hemisphere), whose names abbreviations and locations are listed in Table A-I-1.

The value of f min increases by the solar corpuscle bombardment on the lower ionosphere, and sometimes all ionospheric echoes are completely absorbed by unusual ionization (f min $\equiv B$). Thus Δf min (the deviation of f min value from the monthly median) is used to analyse the polar blackouts.

Table A-I-1. Ionospheric sounding stations

Ionospheric station	Abbr.	Geomagnetic		Corr. Geomagnetic	
		Lat.	Long.	Lat.	Long.
Thule, Greenland	TH	88.1	1.1	(86.2)	(25.6)
Eureka, Canada	EU	86.5	236.0	88.8	252.1
Alert, Canada	AL	85.0	168.5	86.1	132.7
Fletchers Ice, Canada (drifting)	FL	(83.6)	(222.0)	(86.1)	(224.0)
Resolute Bay, Canada	RE	83.0	289.4	84.2	303.2
Clyde River, Canada	CY	81.9	0.5	81.2	16.3
Godhavn, Greenland	GH	79.8	32.7	77.8	42.4
Arctica II, USSR (drifting)	A II	(77.0)	(190.0)	(80.4)	(186.1)
Longyearbyen, Norway	LG	74.4	131.0	74.6	115.1
Baker Lake, Canada	BK	73.7	315.2	75.0	318.7
Tikhaya Bay, USSR	TI	71.5	153.2	74.3	140.3
Narsarssuak, Greenland	NR	71.2	37.6	69.3	44.6
Reykjavik, Iceland	RY	70.1	71.1	66.6	70.6
Yellowknife, Canada	YN	69.0	293.3	69.8	293.1
Churchill, Canada	CC	68.7	322.8	70.2	324.4
Point Barrow, USA	PO	68.5	241.2	69.4	246.2
Arctica I, USSR (drifting)	AI	(68.0)	(209.0)	(71.2)	(214.3)
Tromsø, Norway	TS	66.9	116.2	66.0	104.5
Kiruna, Sweden	KR	65.3	115.6	64.4	104.3
Fairbanks, USA	FA	64.6	256.6	64.6	259.4
Murmansk, USSR	MR	64.1	126.4	64.6	114.1
Sodankylä, Finland	SD	63.8	120.1	63.5	108.4
Dixon Is., USSR	DX	63.0	161.5	67.9	154.0
Luleå, Sweden	LU	62.9	114.7	61.9	104.0
Lycksele, Sweden	LY	62.5	110.8	61.0	100.7
Meanook, Canada	ME	61.8	300.7	62.3	299.4
Anchorage, USA	AN	60.9	258.2	60.5	260.4
Inverness, UK	IV	60.7	83.4	56.9	80.1
Kjeller, Norway	KJ	60.0	100.2	57.3	92.6
Providence Bay, USSR	PV	59.7	235.6	60.3	240.7
Winnipeg, Canada	WI	59.6	322.7	61.0	321.9
Upsala, Sweden	UP	58.5	106.0	56.5	97.4
St. John's, Newfoundland	ST	58.4	21.4	58.5	28.7
Nurmijärvi, Finland	NU	57.8	112.6	56.7	104.0
Ottawa, Canada	OT	56.9	351.5	59.1	354.4
Salekhard, USSR	SH	56.4	148.5	60.8	139.4
Juliusruh, Germany	JU	54.5	98.6	51.4	92.0
Slough, UK	SL	54.3	84.1	50.1	81.0
Victoria, Canada	VI	54.3	293.4	53.9	291.9
De Bilt, Netherlands	DE	53.7	89.5	49.7	85.0
Lindau, Germany	LI	52.1	93.9	48.4	88.6
Dourbes, Belgium	DO	51.9	87.6	47.7	83.8
Fort Monmouth, USA	FM	51.7	353.9	54.0	356.2
Yakutsk, USSR	YK	51.0	193.8	56.4	198.1
Moscow, USSR	MO	50.8	120.6	50.9	111.1
Washington, USA	WS	50.0	350.3	52.3	351.6
Poitiers, France	PS	49.5	81.8	44.7	79.5
Sverdlovsk, USSR	SV	48.5	140.7	52.2	132.1
Freiburg, Germany	FI	48.4	90.0	43.9	85.8
Schwarzenburg, Suisse	SW	48.0	88.7	43.4	84.9

Ionospheric station	Abbr.	Geomagnetic		Corr. Geomagnetic	
		Lat.	Long.	Lat.	Long.
Adak, USA	AD	47.2	240.1	46.7	241.8
Graz, Austria	GZ	46.9	97.0	43.1	91.5
Budapest, Hungary	BP	46.6	100.6	43.2	94.4
Tomsk, USSR	TM	45.9	159.6	52.3	155.0
Monte Capellino, Italy	MT	45.8	89.6	41.0	85.7
San Francisco, USA	SF	43.6	298.6	42.5	297.1
Rome, Italy	RO	42.5	92.0	37.6	87.9
Simferopol, USSR	SM	41.2	113.3	39.6	106.1
White Sands, USA	WH	41.0	316.4	40.4	314.4
Rabat, Morocco	RB	38.7	69.9	32.2	70.7
Grand Bahama, USA	GR	37.9	349.3	40.0	348.8
Sakhalin Is., USSR	SK	36.9	207.5	40.5	213.0
Wakkanai, Japan	WA	35.2	206.1	39.0	210.8
Alma-Ata, USSR	AA	33.5	150.8		
Ashkhabad, USSR	AS	30.6	133.5		
Akita, Japan	AK	29.4	205.5		
Tokyo, Japan	TO	25.4	205.5		
Daker Sénégal	DK	21.8	54.6		
Maui, USA	MU	20.8	268.2		
Panama Canal Zone, Canal Zone	PN	20.6	348.6		
Yamagawa, Japan	YA	20.3	197.9		
Delhi, India	DH	18.8	149.0		
Paramaribo, Surinam	PB	17.0	15.3		
Bogota, Colombia	BG	16.0	354.5		
Okinawa, Liu Kiu	OK	15.2	195.7		
Ahmedabad, India	AH	14.1	143.8		
Taipei, Formosa	TA	14.0	189.0		
Calcutta, India	CT	12.2	158.8		
Ibadan, Nigeria	IB	10.6	74.8		
Bombay, India	BM	9.8	143.8		
Djibouti, French Somaliland	DJ	7.0	113.5		
Talara, Peru	TL	6.6	347.7		
Baguio, Philippines	BA	5.0	189.3		
Bangui, Africa France	BU	5.0	88.6		
Chiclayo, Peru	CL	4.4	349.2		
Madras, India	MA	3.3	150.3		
Chimbote, Peru	CB	2.2	350.4		
Tiruchirapalli, India	TP	1.3	148.3		
Kodaikanal, India	KD	0.7	147.5		
Trivandrum, India	TV	-0.1	146.3		
Huancayo, Peru	HU	-0.6	353.8		
La Paz, Bolivia	LP	-5.0	0.9		
Singapore, Malaya	SG	-10.0	172.7		
Hollandia, New Guinea	HL	-12.6	210.3		
São Paulo Brazil	SO	-12.9	21.0		
Tucuman, Argentine	TU	-15.3	3.3		
Tsumeb, S. Africa	TB	-18.3	82.8		
Salisbury, Phodesia	SY	-19.5	96.2		
Rarotonga, Pacific Ocean	RA	-20.9	273.8		
Buenos-Aires, Argentine	BE	-23.3	9.4		

Ionospheric station	Abb.	Geomagnetic		Corr. Geomagnetic	
		Lat.	Long.	Lat.	Long.
Tananarive, Madagascar	TN	-23.7	112.6		
Concepcion, Chile	CO	-25.3	356.5		
Johannesburg, S. Africa	JO	-26.9	91.4		
Townsville, Australia	TW	-28.4	219.0		
Capetown, S. Africa	CP	-32.7	79.7		
Brisbane, Australia	BR	-35.8	226.9	-36.6	225.6
Port Stanley, Falkland Is.	PY	-40.4	9.0	-36.0	11.3
Watheroo, Australia	WT	-41.7	185.8	-42.5	184.0
Ushuaia, Argentine	US	-43.3	0.8	-39.3	5.1
Canberra, Australia	CN	-43.8	223.7	-45.2	222.0
Godley Head, New Zealand	GD	-48.1	252.8	-50.8	253.0
Deception, Antarctica	DC	-51.6	6.1	-47.4	10.6
Hobart, Australia	HB	-51.7	224.6	-53.9	222.6
Port Lockroy, Antarctica	PL	-53.4	3.9	-49.3	9.2
Kerguelen, Indian Ocean	KG	-57.2	128.0	-57.8	122.5
Campbell Is., New Zealand	CM	-57.4	253.1	-60.7	254.2
Macquarie Is., Southern Ocean	MQ	-61.1	243.1	-64.6	243.0
Halley Bay, Antarctica	HY	-65.8	24.3	-61.2	27.9
Ellsworth, Antarctica	EL	-66.9	14.7	-62.4	21.0
Byrd Station, Antarctica	BY	-70.6	336.1	-69.0	351.9
Mawson, Antarctica	MW	-73.1	103.0	-70.4	92.0
Little America, Antarctica	LA	-74.0	312.0	-74.4	332.3
Cape Hallet, Antarctica	CH	-74.6	278.1	-77.9	294.1
Terre Adelie, Antarctica	TE	-75.3	233.4	-80.1	226.8
Wilkes, Antarctica	WL	-77.9	178.8	-79.6	155.1
Scott Base, Antarctica	SC	-79.0	294.4	-80.7	323.0

(Note) For the higher latitude stations ($|\Phi_m| > 35^\circ$), the corrected geomagnetic coordinates are calculated in accordance with the Hultqvist's table (1958) which gives the displacements of the "landing points" of geomagnetic field lines, due to the four spherical harmonic terms following the dipole term (for further details, see Hakura, 1964).

Table A-I-2 Riometer Stations

Name	Abbr.	Freq.	Geomagnetic		Corrected g. m. lat.	Source
			Lat.	Long.		
Churchill	CC	30.0	68.7	322.8	70.2	Jelly Axford-Reid
Fort Yukon	FY	27.6	66.7	257.1	66.7	Leinbach
Fairbanks	FA	27.6	64.6	256.6	64.6	Leinbach
Kingsalmon	KS	27.6	57.5	254.9	57.1	Leinbach
Sampson	SP	18.0	54.0	293.4	53.6	Obayashi- Jacobs
Unalaska	UA	27.6	50.9	247.9	50.0	Leinbach

Appendix I

Table A-I-3. Geomagnetic observatories

Observatory	Abbr.	Geomagnetic		Geographic		ψ	D- ψ
		Lat. ϕ	Long. Λ	Lat. φ	Long. λ		
Thule	Th	88.0	0.0	77.5	291.0	0.0	--79.7
Resolute Bay	Re	83.0	289.0	74.7	265.5	46.5	-140.5
Godhavn	Go	79.8	32.5	69.2	306.5	-17.5	-34.8
Marchison Bay		75.2	137.2	80.0	18.3		
Baker Lake	BL	73.7	315.3	64.3	264.0		
Churchill	Ch	68.7	322.7	58.8	265.9		
Point Barrow	PB	68.6	241.0	71.3	203.2	33.0	- 6.5
Tromsø	Tr	67.1	116.7	69.7	18.9	-30.8	29.7
Cape Chelyuskin	CC	65.9	117.5	77.7	104.3	- 2.3	25.4
College	Co	64.5	255.4	64.9	212.2	27.5	1.9
Big Delta	BD	64.3	259.3	64.0	214.3	26.5	3.3
Murmansk	Mm	64.1	126.5	69.0	33.0	-26.6	38.0
Healy	He	63.6	256.6	63.9	211.1	26.2	1.8
Dickson	Di	63.0	161.5	73.5	80.4	-12.8	41.8
Lerwick	Le	62.5	88.6	60.1	358.8	-23.6	13.7
Dombås	Do	62.3	100.0	62.1	9.1	-23.6	17.6
Anchorage	An	60.9	258.1	61.2	210.1		
Tiksi	Ti	60.5	191.4	71.7	128.9	7.2	7.4
Sitka	Si	60.0	275.4	57.1	224.7	21.4	7.8
Eskdalemuir	Es	58.5	82.9	55.2	356.8	-20.4	9.7
Lovö	Lo	58.1	105.8	59.4	17.8	-22.1	22.6
Rude Skov	RS	55.8	98.5	55.8	12.5	-20.6	18.1
Hartland	Ha	54.6	79.0	51.0	355.5	-18.1	9.1
Yakutsk	Ya	51.0	193.8	62.0	129.7	5.8	-13.1
Fredericksburg	Fr	49.6	349.9	38.2	282.6	2.6	- 9.8
Obessa	Od	43.8	111.1	46.8	30.9	-15.7	17.6
San Fernando	SF	41.0	71.3	36.5	353.8	-13.6	22.6
Tucson	Tu	40.4	312.2	32.3	249.2	10.1	3.2
Tifilisi	Tf	36.7	122.1	42.0	44.7	-13.1	18.3
Memambetsu	Mb	34.1	208.3	43.9	144.2	7.5	-15.7
San Juan	SJ	29.9	3.2	18.4	293.9	- 0.7	- 6.6
Kakioka	Ka	26.0	206.0	36.2	140.2	6.2	-12.6
Honolulu	Ho	21.1	266.5	21.3	201.9	12.3	- 0.7
Kanoya	Ky	20.7	198.1	31.4	150.9	4.2	- 9.2
Guam	Gu	3.9	212.8	13.5	144.8	6.4	- 4.6

(Note) ψ The angle formed by the great circle joining the station and the geomagnetic pole with the geographical meridian of the station (eastward positive) ;

D Declination (for February 1958).

$$\Delta f \text{ min} = f \text{ min} - \overline{f \text{ min}}$$

$\overline{f \text{ min}}$: monthly median of $f \text{ min}$

The region of complete blackout is hatched in the figures.

(ii) Cosmic noise absorption

When the detailed profile of ionization is needed in the present analysis, the cosmic noise absorption is examined for 6 stations listed below.

(iii) Geomagnetic data

In order to draw the current systems, there are used the normal magnetograms and hourly values of three components of 35 geomagnetic stations in the northern hemisphere. The names, abbreviations and locations of those observatories are given in Table A-I-3.

APPENDIX II Method of obtaining Dst and DS variations of geomagnetic storm.

Generally, the disturbance variation (D) is divided into two distinguishable parts as follows :

$$D = Dst + DS$$

where Dst is the storm-time variation, whereas DS shows the local-time variation.

For a geomagnetic storm, Dst (X_m -or Y_m -component) at a latitude Φ is denoted by (Dst Φ) X or Y . In the present analysis, (Dst 32.5) X and Y are obtained as the averages of both components at 6 middle-latitude stations, i.e. San Juan, San Fernando, Tbilisi, Kakioka, Honolulu, and Tucson, where Sq-variations are removed. Since the mean latitudinal distribution of Dst is known from Chapman and Sugiura (1959), an estimation of Dst Φ is given by

$$Dst \Phi = \frac{A(\Phi)}{A(32.5)} Dst^{32.5}$$

where $A(\Phi)$ means the relative factor of the Dst distribution at latitude Φ .

$DS(X_m$ -or Y_m -component) is defined for each station of latitude Φ , as

$$\Delta X_m = X_m - (Dst\Phi)X,$$

or

$$Y_m = Y_m - (Dst\Phi)Y.$$

In Fig. 3-(a)-(h), DS-field of geomagnetic storm is expressed by equivalent current system, where the electric current between successive lines is 1×10^5 amps.

1958年2月11日の極磁気嵐と極冠帯 異常電離について

永井正男 (地磁気観測所)

羽倉幸雄 (電波研究所)

概 要

1958年2月11日の極磁気嵐と極冠帯異常電離について解析した結果、次に示すような特徴的な事柄が明らかになった。

(1) 10日の12時00分に極光帯の昼側で急激な異常電離 (PCA)_A が始まった。そして1~2時間後に極光帯の全ての領域を取りまいて発達した。その後はゆつくりと発達し、11日の01時26分におこった急始変化 (SC1) の直前では極冠帯および極光帯の全領域をおよぐに至った。

同時に急始変化の13時間前から極磁気嵐が始まり、異常電離の発達にもなって次第に活動的になった。この擾乱は通常の Dst 場がきわめて小さいこと、および擾乱の生因が極の電離層に異常電離を起した高エネルギーの太陽宇宙線の侵入と直接関連づけられるために特別な擾乱であると考えてよい。この擾乱を DP (Pre SC) という記号であらわす。

12時30分には永田および国分によってえられた S_p^2 の電流系から、DP (Pre SC) の電流系への移行が見られた。いずれの電流系も、午前の側では時計廻り、午後の側では反時計廻りで同じ型を示すが、 S_p^2 場が極冠帯に限られるのに反して、DP (Pre SC) 場は極光帯の夜側で増大が見られるのが特徴的である。

(2) 極冠帯の全域にわたって急始変化 (SC1) のすぐ直前に電離の異常増大が見られた ((PCA) pre SC) これは Axford-Reid が述べている惑星空間における微粒子流の2つの衝撃波による加速機構と同じ原因によるものと考えられる。

電離層の数多くの資料の解析から侵入粒子の衝突領域に関する進歩したパターンがえられた。侵入粒子のフラックス密度の増大につれて、衝突領域の北限は明らかに地磁気北極の方向へ移動した。一方南限はほとんど変動せずに約 60° の緯度にとどまった。

(3) 2月11日の01時26分と01時59分における引き続いて起った急始変化 (SC1 及び SC2) の電流系が示された。SC1 の電流系は多くの研究者によってえられた電流系とほとんど同じ型を示すが、通常の急始に比べ電流は大きく又 D_s^2 場が極光帯においてかなり拮がっているのが見られた。極冠帯の中心を流れる平行電流は地磁気地方時において20時から08時の方向へ流れた。一方、SC2 における電流系は SC1 における電流系と D_s^2 場の向きが全く反対であった。すなわち午前の例では反時計廻りを示し、午後の側では時計廻りを示して、極冠帯の中心を流れる平行電流は09時から21時の方向へ流れた。これは永田と阿部によってえられた SC* の電流系と、電流の大きさは非常に異なるが、向きはほとんど同じである。

これら2つの急始変化と一致して極冠帯ブラック・アウトの領域も又2段階の膨張が見られた。補正した地磁気座標を用いて、極冠帯ブラック・アウト領域における境界の変動と異常電離領域の緯度変化が詳細に解析された。その結果、2段階に示される異常電離は Brown などによって報告されている急始異常電離の一種と考えられる (SCA 1 および SCA 2)。急始異常電離の原因は、地磁気急始変化に対応する2つの衝撃波の影響によってしぼり出された Van Allen 帯からの電子降下に帰せられる。この想像は同時に観測された亜極光帯の烈しいオーロラの出現によっても支持される。

- (4) 極冠帯の中心部を流れる平行電流の向きについて、Thuleにおける毎時値を使って、急始を中心に-24時間から+24時間まで解析がなされた。-12時間から-1時間までの DP (Pre SC) においては平行電流の向きは08時~13時を示した。又+3時間から+7時間までの Dst 場の発達過程においては07時~08時の朝方に偏した時間を示した。一方+10時間から+18時間までの Dst 場の回復過程においては午前の側から午後の側へ次第に移行し11~13時を示した。すなわち極冠帯の中心部を流れる平行電流の向きは水平ベクトルの大きさには無関係で、Dst 場の発達過程では朝方に偏し、回復過程では次第に午後の例へ移行することがわかった。